British Journal of Pharmacology

DOI:10.1111/bph.13240
www.brjpharmacol.org

RESEARCH PAPER

Synergistic effect of targeting the epidermal growth factor receptor and hyaluronan synthesis in oesophageal squamous cell carcinoma cells

I Kretschmer, T Freudenberger, S Twarock and J W Fischer

Institut für Pharmakologie und Klinische Pharmakologie, Universitätsklinikum der Heinrich-Heine-Universität, Düsseldorf, Germany

Correspondence
Jens W. Fischer, Institut für Pharmakologie und Klinische Pharmakologie, Universitätsklinikum der Heinrich-Heine-Universität Düsseldorf, Moorenstrasse 5, 40225 Düsseldorf, Germany. E-mail: jens.fischer@uni-duesseldorf.de

Received
26 November 2014
Revised
5 June 2015
Accepted
26 June 2015

BACKGROUND AND PURPOSE

Worldwide, oesophageal cancer is the eighth most common cancer and has a very poor survival rate. In order to identify new tolerable treatment options for oesophageal squamous cell carcinoma (ESCC), erlotinib was tested with moderate efficacy in phase I and II studies. As 4-methylumbelliferone (4-MU), an hyaluronan (HA) synthesis inhibitor showed anti-cancer effects *in vitro*, and in ESCC xenograft tumours, we investigated whether the anti-cancer effects of erlotinib could be augmented by combining it with 4-MU.

EXPERIMENTAL APPROACH

ESCC cell lines were treated with erlotinib or gefitinib (1 μmol·L^{-1}) and 4-MU (300 μmol·L^{-1}), and the cell count, cell cycle progression and migration were determined as compared to the single agents and the solvent-control.

KEY RESULTS

The combination of erlotinib and 4-MU synergistically inhibited the proliferation of ESCC cell lines. Furthermore, the migration speed of ESCC cell line KYSE-410 in gap closure assays was significantly reduced by the combination of erlotinib and 4-MU. Decreased ERK phosphorylation could explain the anti-proliferative and anti-migratory effects in the combined treatment group. Finally, the combination was additionally able to decrease the growth of multicellular tumour spheroids, a three-dimensional cell culture model that was associated with sustained inhibition of ERK1/2 phosphorylation.

CONCLUSIONS AND IMPLICATIONS

The combination of 4-MU and erlotinib showed promising anti-cancer efficacies in the ESCC cell lines.

Abbreviations

2D, two dimensional; 3D, three dimensional; 4-MU, 4-methylumbelliferone; CI, combination index; EAC, oesophageal adenocarcinoma; ESCC, oesophageal squamous cell carcinoma; HA, hyaluronan; HAS, hyaluronan synthase; MCTS, multicellular tumour spheroid; qPCR, quantitative real-time PCR; RHAMM, receptor for HA-mediated motility

Tables of Links

TARGETS	
Catalytic receptors[a]	**Enzymes**[b]
EGFR	Akt (PKB)
ErbB2 (HER2)	ERK
TGFR (TGFBR1)	PI3K

LIGANDS	
AG 1024	Gefitinib
Cetuximab	Gemcitabine
Erlotinib	Hyaluronan (HA)
Fluvastatin	Sorafenib
	Trastuzumab

These Tables list key protein targets and ligands in this article which are hyperlinked to corresponding entries in http://www.guidetopharmacology.org, the common portal for data from the IUPHAR/BPS Guide to PHARMACOLOGY (Pawson *et al.*, 2014) and are permanently archived in the Concise Guide to PHARMACOLOGY 2013/14 ([a,b]Alexander *et al.*, 2013a,b).

Introduction

Oesophageal cancer accounted for 3.2% of new cancer cases in 2012. It is therefore the eighth most frequently diagnosed type of cancer and the sixth most common cause of cancer deaths (approx. 400 000 per year). The very poor survival prognosis for patients suffering from this cancer entity is defined by an overall ratio of mortality to incidence of 0.88 (Ferlay *et al.*, 2015). The two major types of oesophageal cancer are squamous cell carcinoma (ESCC) and adenocarcinoma (EAC). Treatment of oesophageal cancer depends upon type, stage, location of the tumour and on the medical condition of the patient. The treatment of ESCC comprises surgery and/or chemoradiation with platinum derivatives and 5-fluorouracil or taxanes (Stahl *et al.*, 2013). In the past years, new targeted therapies for epithelial tumours such as receptor TK inhibitors have been investigated in anti-cancer studies.

To date, there are few clinical phase I and II trials on the efficacy of treatments including the EGFR TK inhibitor erlotinib in oesophageal cancer. In the studies on the treatment of ESCC, progression-free survival ranged from 3.3 to 12 months (Ilson *et al.*, 2011; Zhai *et al.*, 2013). The most prominent adverse effects of erlotinib were diarrhoea and rash (Dragovich *et al.*, 2006; Ilson *et al.*, 2011). Most authors did not report a significant correlation of EGFR expression level and treatment outcome due to small sample sizes (Ilson *et al.*, 2011; Iyer *et al.*, 2013; Zhai *et al.*, 2013). However, the efficacy of erlotinib might be better in the treatment of ESCC compared to EAC. In ESCC, EGFR overexpression was more frequently detected (Ilson *et al.*, 2011; Fichter *et al.*, 2014). In ESCC cell lines, the combination of erlotinib with cetuximab, a monoclonal antibody directed against the EGFR, or the combination of erlotinib with the tyrphostin AG 1024, an insulin-like growth factor receptor TK inhibitor, or fluvastatin, was shown to have additive or even synergistic antiproliferative effects (Sutter *et al.*, 2006).

Hyaluronan (HA), a major component of the extracellular matrix, is found in the tumour stroma and parenchyma of ESCC, depending upon the degree of tumour differentiation (Wang *et al.*, 1996). We previously showed that HA synthase (HAS) isoform 3 mRNA expression was up-regulated in human ESCC tissue samples compared with normal mucosa (Twarock *et al.*, 2011). Tumour cell-associated HA is associated with poor prognosis in breast cancer (Auvinen *et al.*, 2000; 2013), colorectal cancer (Ropponen *et al.*, 1998), pancreatic cancer (Cheng *et al.*, 2013) and malignant peripheral nerve sheath tumours (Ikuta *et al.*, 2014). Inhibition of HA synthesis by 4-methylumbelliferone (4-MU) and HAS3 knockdown leads to decreased tumour volume in ESCC xenograft tumours in nude mice, and similarly, 4-MU treatment reduces tumour volume in a prostate cancer xenograft model (Lokeshwar *et al.*, 2010). Additionally, 4-MU inhibited metastases in several animal studies (Yoshihara *et al.*, 2005; Arai *et al.*, 2011; Okuda *et al.*, 2012; Hiraga *et al.*, 2013). First examples for combining inhibition of HA synthesis with other anti-cancer drugs are the combinations with gemcitabine (Nakazawa *et al.*, 2006), with the multi-kinase inhibitor sorafenib (Benitez *et al.*, 2013) and with trastuzumab, a recombinant humanized anti-ErbB2 antibody (Palyi-Krekk *et al.*, 2007). However, no information is available about increasing the effect of 4-MU in ESCC by additional chemotherapeutic drugs.

It has been shown previously that EGFR mRNA expression correlated with HAS3 mRNA expression in human ESCC tissue samples. In OSC1 cells, an ESCC cell line, EGF stimulation induced HAS3 mRNA expression pointing towards a role of HA in EGFR-regulated processes (Twarock *et al.*, 2011). In squamous cell carcinoma of the head and neck, HA and EGFRs were expressed in a similar way (Jonsson *et al.*, 2012). It is noteworthy that HA binding to its receptor CD44 promoted association with and activation of the EGFR (Toole, 2009). Activation of both EGFR and CD44 by their ligands induces downstream signalling pathways such as MAPK/ERK and PI3K/Akt and promotes proliferation, migration and survival (Citri and Yarden, 2006; Toole, 2009). The present experiments show that combining erlotinib and 4-MU resulted in significant inhibition of proliferation and migration of the ESCC cell line KYSE-410.

Methods

Cell culture, drugs and siRNA transfection

The human ESCC cell lines KYSE-270, KYSE-410 and KYSE-520 were purchased from the Leibnitz Institute DSMZ – German Collection of Microorganisms and Cell Cultures (Braunschweig, Germany) (Shimada *et al.*, 1992). Cells were grown in RPMI 1640 GlutaMAX™ medium (Gibco®, Life

Technologies™, Paisley, UK) supplemented with 1% penicillin-streptomycin (Gibco, Life Technologies) and 10% fetal calf serum (Gibco, Life Technologies) in a humidified atmosphere at 37°C and 5% CO_2. If not stated otherwise, cells were treated with 1 μmol·L^{-1} erlotinib or gefitinib (both LC Laboratories, Woburn, MA, USA) and 300 μmol·L^{-1} 4-methylumbelliferone sodium salt (Sigma, Steinheim, Germany), all dissolved in DMSO (Carl Roth GmbH, Karlsruhe, Germany). For knockdown of the HA receptors, the following FlexiTube siRNAs (Qiagen, Hilden, Germany) were used: siCD44 (Hs_CD44_5); siRHAMM (Hs_HMMR_9); control (Ctrl_AllStars_1). Cells were transfected in the culture medium free of antibiotics using Lipofectamine® RNAiMAX Transfection Reagent (Invitrogen™, Life Technologies™, Carlsbad, CA, USA), according to the manufacturer's protocol for 'reverse transfection'. After 24 h, the medium was replaced by growth medium supplemented with 1 μmol·L^{-1} erlotinib or DMSO.

RNA isolation, cDNA synthesis and quantitative real-time PCR (qPCR)

RNA was isolated by peqGOLD TriFast™ (Peqlab, Erlangen, Germany)/chloroform, and its concentration and purity were determined by spectrophotometry (Nanodrop, Thermo Scientific, Wilmington, DE, USA). Subsequent reverse transcription was carried out using the QuantiTect® Reverse Transcription Kit (Qiagen, Hilden, Germany). qPCR was performed in duplicate on the StepOnePlus™ Real-Time PCR System (Life Technologies) using the Platinum® SYBR® Green qPCR SuperMix-UDG (Life Technologies) with ROX reference dye according to the manufacturer's protocol. The sequences of the primers are listed in Table 1 (Rogojina *et al.*, 2003; Twarock *et al.*, 2009; 2010; Röck *et al.*, 2012). Data were analysed by the ΔΔCq method using GADPH as a reference gene.

Cell count and determination of synergism

Cells were seeded at 5000 cm^{-2} in 12-well plates. After 24 h, the medium was changed and erlotinib or gefitinib at final concentrations of 0.25, 0.5, 1, 2 and 4 μmol·L^{-1} as well as 4-MU at final concentrations of 50, 75, 150, 300 and 600 μmol·L^{-1} were added alone or in combination at a ratio of 1:300 in five dilutions beginning with 0.167 μmol·L^{-1} erlotinib plus 50 μmol·L^{-1} 4-MU to 2 μmol·L^{-1} erlotinib plus 600 μmol·L^{-1} 4-MU. After an additional 72 h, cells were trypsinized and counted in a Neubauer chamber. The effect of each dose was calculated by counting the number of cells compared with the control-treated wells. In order to obtain a linear regression coefficient of $r \geq 0.95$ appropriately, the average effects of at least five independent experiments were used to simulate the median-effect plots of the drugs as single agents or in combination and to subsequently determine the combination index (CI) using the CompuSyn Software (Chou and Martin, 2005) as described by Chou (2006).

Cell cycle analysis

Cells were seeded and treated as described earlier. After trypsinization, cells were washed with PBS and permeabilized using 75 μL of 0.1% sodium citrate solution (Carl Roth GmbH) containing 0.1% Triton X-100 (Sigma, St. Louis, MO, USA) as described by Nicoletti *et al.* (1991). Subsequently, 25 μL of Guava® Cell Cycle Reagent (EMD Millipore Corporation, Hayward, CA, USA) was added and DNA content was measured on the Guava easyCyte™ Flow Cytometer (EMD Millipore Corporation). Histogram deconvolution was performed by ModFit LT™ Software (Verity Software House, Topsham, ME, USA).

[^{3}H]-thymidine proliferation assay

One day after seeding, cells were incubated with 4-MU, erlotinib or vehicle for 24 h, and [^{3}H]-thymidine (Perkin Elmer, Waltham, MA, USA) was added for the last 6 h at a final concentration of 0.5 μCi·mL^{-1} and specific activity of 2 Ci·mmol^{-1}. After the cell layer had been washed with cold PBS, it was harvested by 0.3 mol·L^{-1} perchloric acid and 0.1 mol·L^{-1} sodium hydroxide. After addition of Rotiszint® ecoplus scintillation mix (Carl Roth GmbH), radioactivity was counted in the Beckman LS 6000 IC scintillation counter for 3 min. Counts were normalized to total protein in the lysates, which was quantified by the Bradford method-based Bio-Rad protein assay (Bio-Rad Laboratories, Inc., München, Germany).

Western blot

Cells were lysed in a buffer containing 125 mmol·L^{-1} Tris, 100 mmol·L^{-1} DTT, 20% glycerol, 4% SDS, 100 mmol·L^{-1} NaF,

Table 1

Primer sequences used in qPCR

Gene	Forward (5′–3′)	Reverse (5′–3′)
CD44	GCTATTGAAAGCCTTGCAGAG	CGCAGATCGATTTGAATATAACC
EGFR	GCGTCCGCAAGTGTAAGAAG	TGATGGAGGTGCAGTTTTTG
GAPDH	GTGAAGGTCGGAGTCAACG	TGAGGTCAATGAAGGGGTC
HAS2	GTGGATTATGTACAGGTTTGTGA	TCCAACCATGGGATCTTCTT
HAS3	GAGATGTCCAGATCCTCAACAA	CCCACTAATACACTGCACAC
HYAL1	CCAAGGAATCATGTCAGGCCATCAA	CCCACTGGTCACGTTCAGG
HYAL2	TTCACACGACCCACCTACAG	GTCTCCGTGCTTGTGGTGTA
RHAMM	GAATTTGAGAATTCTAAGCTTG	CCATCATACCCCTCATCTTTGTT

1 μg·mL^{-1} leupeptin, 1 μg·mL^{-1} aprotinin and bromphenol blue. Cell lysates were run on a 10% SDS-PAGE and blotted onto 0.2 μm Whatman™ nitrocellulose membranes (GE Healthcare, Buckinghamshire, UK). Membranes were blocked with 5% BSA in TBS/Tween®20 buffer. Primary antibodies were purchased from Cell Signaling Technology® (Beverly, MA, USA) and diluted at a ratio of 1:1000 (pERK # 9101, ERK # 9102, pAKT # 9271, AKT # 9272). Membranes were incubated with primary antibodies overnight at 4°C followed by 1 h incubation with a secondary antibody (1:5000 dilution of goat anti-rabbit IRDye® 800CW, #926-32211, LI-COR® Biosciences, Lincoln, NE, USA). Monoclonal anti-β-tubulin I antibody (# T7816, Sigma-Aldrich, St. Louis, MO, USA) as primary antibody and goat anti-mouse IRDye® 680LT (# 926-68020, LI-COR Biosciences) as secondary antibody were used to quantify the control. Membranes were scanned and integrated intensities were measured using the Odyssey infrared imaging system (LI-COR Biosciences).

Migration assay

Cells were seeded at 20 000 cells per chamber in ibidi® cell culture inserts composed of two chambers separated by a 500 μm wall. After 24 h, the inserts were removed, resulting in two confluent cell monolayers separated by a defined gap. Medium containing either 1 μmol·L^{-1} erlotinib, 300 μmol·L^{-1} 4-MU, a combination of both or vehicle DMSO was added followed by phase contrast time-lapse microscopy using the 5× objective of the Zeiss AxioObserver Z.1 (Carl Zeiss MicroImaging GmbH, Göttingen, Germany). The addition of 5 mmol·L^{-1} hydroxyurea prevented proliferation of the cells. In the pictures taken every 120 min, the distance between the cell layers was measured using Zen2012 Software (Carl Zeiss MicroImaging GmbH) at the two sites of minimum and maximum distance after 24 h. The difference in the mean distances was divided by 120 min to calculate the gap closing speed within a period of 24 h or until the gap was closed.

ELISA-like HA assay

For quantification of HA in the cell culture supernatants, KYSE-410 were seeded and treated as described earlier. After 24 h of treatment, supernatants were harvested and the amount of HA was determined with the hyaluronic acid test kit (Corgenix, Westminster, CO, USA) and normalized to total protein quantified by the Bradford method, as described previously.

Three-dimensional (3D) cell culture

3D cell culture was carried out as described in Friedrich *et al*. (2009). Briefly, 3000 cells were seeded in 96-well plates coated with 1.5% agarose followed by centrifugation at 200× *g* for 5 min. After 4 days of multicellular tumour spheroid (MCTS) formation, cells were treated with either vehicle, 300 μmol·L^{-1} 4-MU, 1 μmol·L^{-1} erlotinib or the combination of 1 μmol·L^{-1} erlotinib and 300 μmol·L^{-1} 4-MU. MCTS diameter was measured before (day 4) and after 3, 6 and 10 days of treatment (days 7, 10 and 14 after seeding) using phase contrast images taken with a 5× objective of the Zeiss AxioObserver Z.1 and AxioVision Software (Carl Zeiss MicroImaging GmbH).

Statistical analysis

GraphPad Prism 6 Software Version 6.04 (GraphPad Software, Inc., La Jolla, CA, USA) was used for statistical analysis. The relative expression values obtained by qPCR were logarithmically transformed and then compared with the given expression level in the control group by one-sample *t*-test in case of knockdown control and ordinary one-way ANOVA with Sidak's multiple comparison test. MCTS growth curves were analysed by two-way ANOVA (Figure 7B). Western blot data of pERK/ERK and pAkt/Akt were normalized to control samples and Kruskal–Wallis test was performed. Migration assay data did not pass the Kolmogorov–Smirnov normality test and were therefore tested using the Kruskal–Wallis test and Dunn's multiple comparisons test. Likewise, percentage values obtained in the cell cycle analysis experiments were analysed using the Kruskal–Wallis test and Dunn's multiple comparisons test. In other cases, ordinary one-way ANOVA and Sidak's multiple comparisons test were used. All groups were compared with the control group and the combined treatment group. P values < 0.05 were defined as statistically significant.

Results

Combined inhibition of EGFR TK and HA signalling reduced the cell number

In KYSE-410 cells, treatments using either 4-MU or erlotinib or the combination resulted in decreased cell counts (Figure 1A) compared with the control. The combination of both drugs lowered the cell count most effectively and significantly fewer cells were counted compared to the samples treated with single agents. In order to investigate if interfering with HA signalling by knockdown of the two major HA receptor CD44 and receptor for HA-mediated motility (RHAMM) would show the same effect, cells were transfected with siRNA and subsequently treated with erlotinib or vehicle. Samples were transfected in parallel and randomly checked for knockdown efficiency (Figure 1B and D). Erlotinib treatment combined with a knockdown of CD44 significantly reduced the cell number as compared to control and single erlotinib treatment as well as compared to vehicle-treated siCD44 transfected cells (Figure 1C). In contrast, comparing erlotinib treatment of cells with and without knockdown of RHAMM, only a non-significant trend towards a further reduction of the cell number in erlotinib and siRHAMM-treated cells (Figure 1E) was observed. Hence, inhibition of HA synthesis by 4-MU or blocking HA signalling by CD44 knockdown augmented the effect of erlotinib. In contrast to 4-MU treatment, the knockdown of CD44 and RHAMM alone did not significantly reduce the number of cells. However, the combination of 4-MU with knockdown of CD44 caused a further, albeit non-significant, decrease in the cell number (Figure 1F).

Synergistic reduction of cell number by combined erlotinib and 4-MU treatment

To further investigate whether the administration of 4-MU and erlotinib reduced the number of cells in a synergistic or additive way, KYSE-410 were treated with dilutions of erlotinib and 4-MU as single agents or in combination (Figure 2A), and median-effect plots and the CI were calculated. The correlation coefficients of the median-effect plot

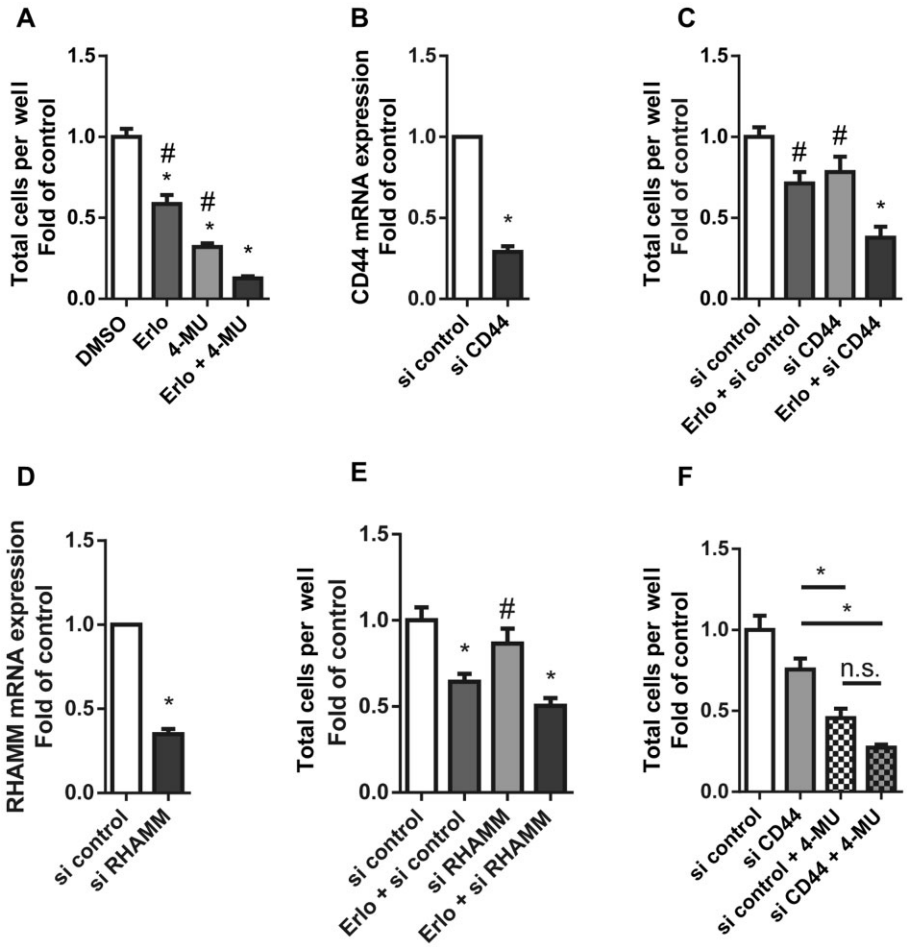

Figure 1

Inhibition of HA signalling in addition to erlotinib treatment significantly reduced the number of cells. (A) Cell count after 72 h of treatment with vehicle, erlotinib, 4-MU or a combination of 4-MU and erlotinib, $n = 5$. (B) CD44 mRNA expression in cells transfected with siCD44, $n = 3$. (C) Cell count of cells either transfected with control siRNA or siRNA targeting CD44 ± erlotinib, or vehicle for 72h, $n = 7$. (D) RHAMM mRNA expression in cells treated with siRNA targeting RHAMM, $n = 4$. (E) Cell count after transfection with siRHAMM or si control and subsequent treatment with erlotinib or vehicle, $n = 7$. *$P < 0.05$ compared with control; #$P < 0.05$ compared with erlotinib + 4-MU or compared with erlotinib + siRNA transfection. (F) Cell count after transfection with siCD44 and subsequent treatment with 4-MU or vehicle, $n = 6$. *$P < 0.05$; n.s., not significant. Data represent mean ± SEM.

were $r = 0.991$ for erlotinib alone, $r = 0.985$ for 4-MU alone and $r = 0.994$ for the combination of erlotinib and 4-MU. The CI values measured for fractions affected (F_a) ≥ 0.5 were in the range of 0.3–0.7, indicating synergism (Figure 2B). The combination additionally reduced the number of KYSE-270 and KYSE-520 cells in a synergistic way (Figure 2C–F) for $F_a \geq 0.5$. Furthermore, another EGFR TK inhibitor, gefitinib, showed synergistic to moderate synergistic effects on KYSE-410 cell number in combination with 4-MU (Supporting Information Fig. S1A and B).

Erlotinib and 4-MU reduced the number of cells in the S-phase

Flow cytometry analysis of propidium iodide-stained cells was subsequently used to elucidate the underlying mechanism of the decreased number of KYSE-410 by 4-MU and erlotinib treatment. No significant increase of cells in the sub-G1 phase was observed after any of the treatments, excluding an effect on apoptosis (Figure 3A). Furthermore, the fraction of cells in the G0/G1 phase increased in the double treatment group (Figure 3B) as compared to erlotinib or vehicle-treated cells alone. Accordingly, after 24 h of treatment, the proportion of KYSE-410 in the S-phase was significantly lower in dual erlotinib and 4-MU-treated cells compared with erlotinib or vehicle-treated cells (Figure 3C and E). An induction of the proportion of cells in the G0/G1 phase as well as a reduced percentage of cells in the S-phase was also observed by combined gefitinib and 4-MU treatment in KYSE-410 cells and by combined erlotinib and 4-MU treatment in KYSE-270 and KYSE-520 cells (Supporting Information Fig. S2). The proportion of cells in the G2/M phase did not increase significantly (Figure 3D). Additionally, KYSE-410 incorporated significantly less [^{3}H]-thymidine when treated

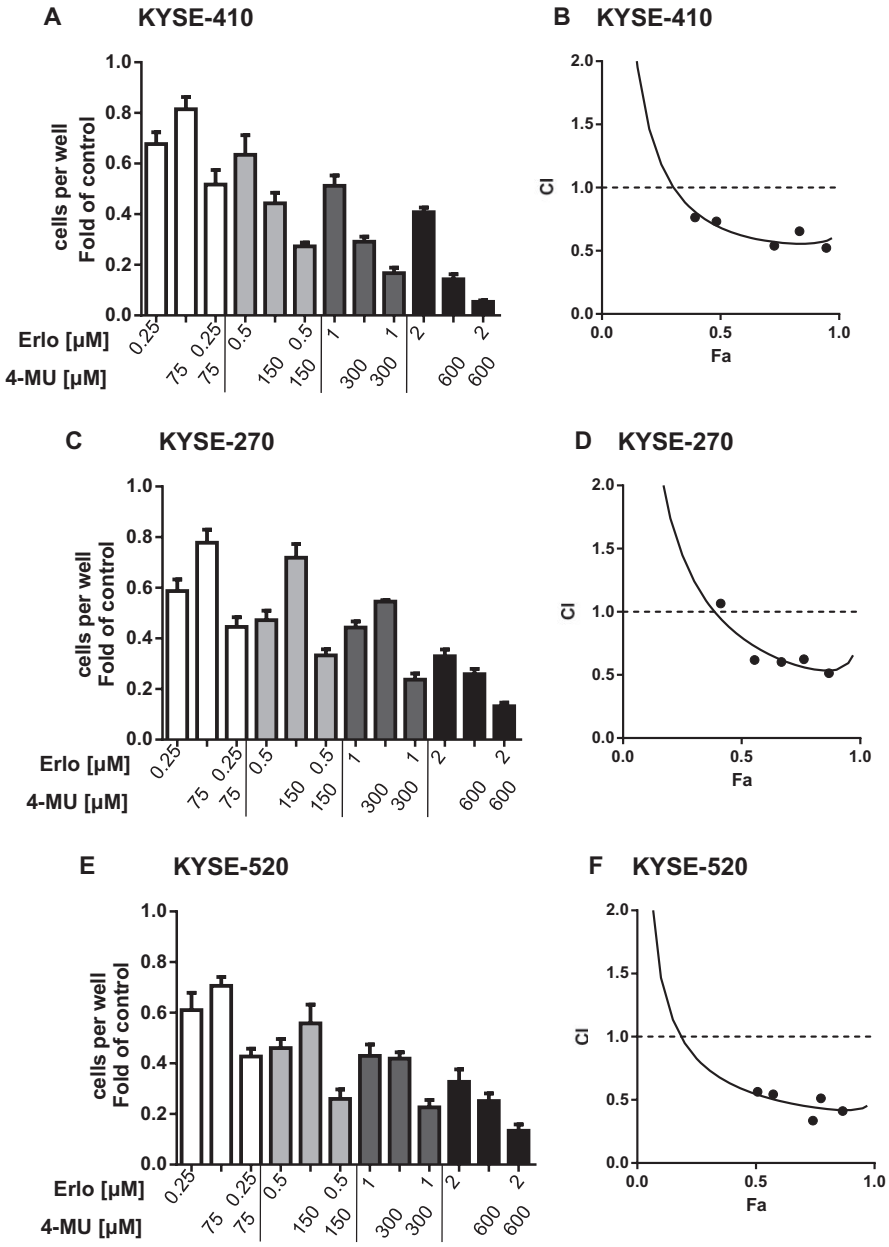

Figure 2

Synergistic action of erlotinib and 4-MU. (A) KYSE-410 cell count after 72 h of treatment with serial dilutions of erlotinib or 4-MU as single agents or in combination, $n = 5$–10. (B) CI values calculated for erlotinib and 4-MU in KYSE-410, $n = 5$. (C) KYSE-270 cell count after 72 h of treatment with serial dilutions of erlotinib or 4-MU as single agents or in combination, $n = 5$. (D) CI values calculated for erlotinib and 4-MU in KYSE-270. (E) KYSE-520 cell count after 72 h of treatment with erlotinib and 4-MU, $n = 5$. (F) CI values calculated for erlotinib and 4-MU in KYSE-520. Data are presented as mean ± SEM. (B, D, F) CI values were calculated from the means of the cell count data by the method of Chou (2006). The line-drawing shows the fitted values and actual values (filled circles).

with combined, 4-MU and erlotinib (Figure 3F), supporting the anti-proliferative effect of the combination.

Phosphorylation of ERK but not Akt was reduced by erlotinib and 4-MU

Western blot analysis of cells harvested after 24 h of treatment showed significantly reduced ERK phosphorylation when treated with erlotinib combined with 4-MU. Additionally, there was a strong trend towards a reduced ERK phosphorylation in KYSE-410 treated with erlotinib alone (Figure 4A and B).

Similar findings were obtained by treating KYSE-270 and KYSE-520 cells with erlotinib and 4-MU (Figure 4E–H) and by gefitinib treatment of KYSE-410 cells (Supporting

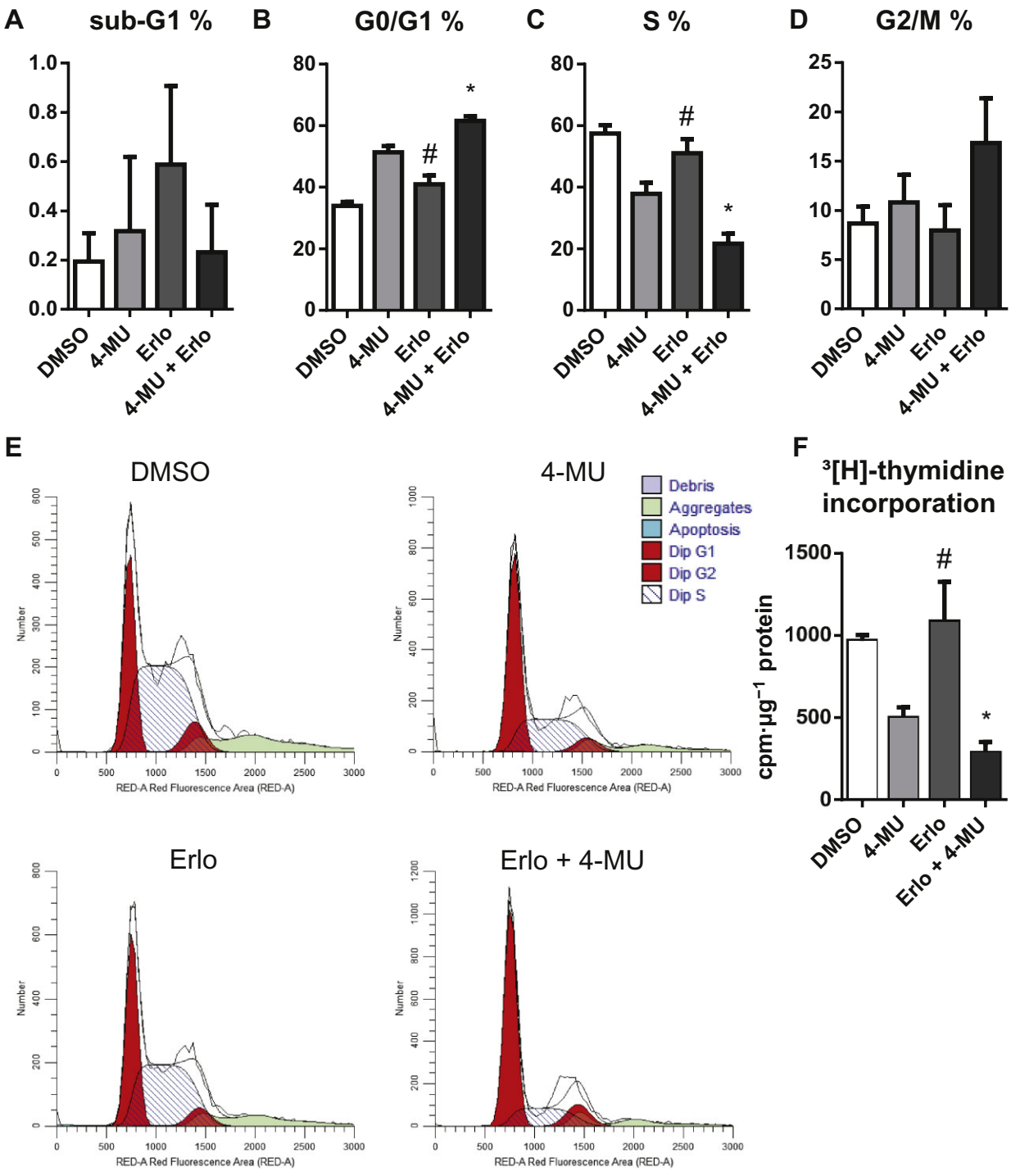

Figure 3

Combined erlotinib and 4-MU treatment reduced the percentage of KYSE-410 in the S-phase. Flow cytometric analysis of propidium iodide-stained cells treated with 4-MU or erlotinib as single agents or in combination for 24 h. The percentages of cells in sub-G1 (A), G0-G1 (B), S (C), G2-M (D) phase are shown, n = 5. (E) Representative histograms of flow cytometric cell cycle analysis and histogram deconvolution. (F) [^{3}H]-thymidine incorporation after 24 h of treatment with erlotinib and 4-MU alone or in combination, n = 5. Data are presented as mean ± SEM; *P < 0.05 compared with control; #P < 0.05 compared with erlotinib + 4-MU.

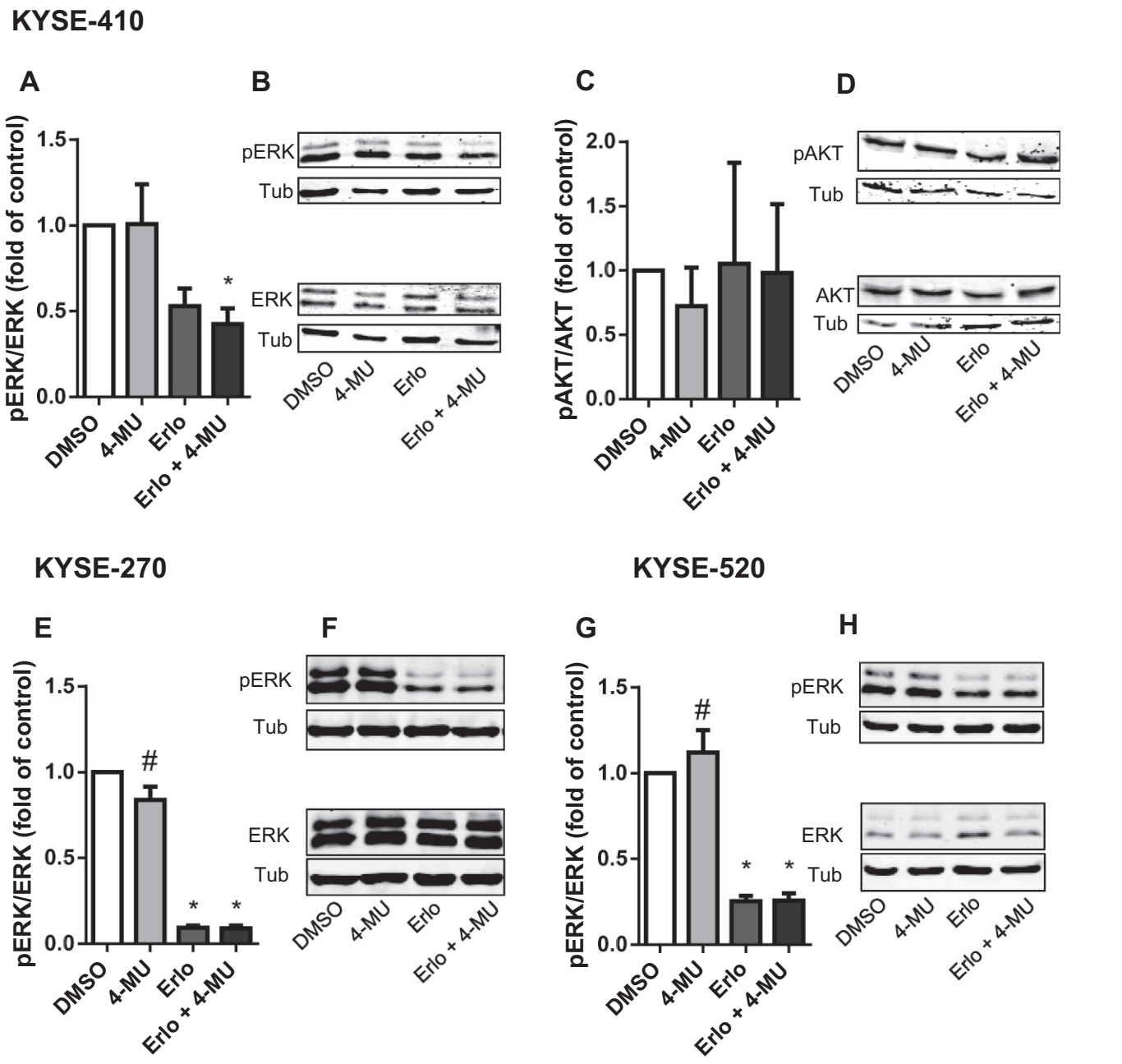

Figure 4

Erlotinib and combined erlotinib and 4-MU treatment inhibited ERK phosphorylation in ESCC cells. (A) Western blot analysis of phosphorylated ERK in relation to total ERK in KYSE-410 after 24 h of treatment with erlotinib and 4-MU, $n = 7$. (B) Representative blots of phosphorylated and total ERK and β-tubulin loading control in lysates of KYSE-410. (C) Western blot analysis of phosphorylated Akt in relation to total Akt in KYSE-410 after 24 h of treatment, $n = 6$. (D) Representative blots of phosphorylated and total Akt and β-tubulin loading control in lysates of KYSE-410. (E) Western blot analysis of phosphorylated ERK in relation to total ERK in KYSE-270 after 24 h of treatment with erlotinib and 4-MU, $n = 7$. (F) Representative blots showing phosphorylated and total ERK and β-tubulin loading control in lysates of KYSE-270. (G) Western blot analysis of phosphorylated ERK in relation to total ERK in KYSE-520 after 24 h of treatment with erlotinib and 4-MU, $n = 7$. (H) Representative blots showing phosphorylated and total ERK and β-tubulin loading control in lysates of KYSE-520. Data are presented as mean ± SEM; $^*P < 0.05$ compared with control; $\#P < 0.05$ compared with erlotinib + 4-MU.

Information Fig. S1C and D). In these cases, the receptor TK inhibitors alone were able to significantly reduce ERK phosphorylation. Furthermore, treating KYSE-410 with erlotinib and erlotinib combined with 4-MU resulted in a significantly reduced ERK phosphorylation even after 20 min. At this time point, 4-MU treatment resulted in a trend towards decreased ERK phosphorylation as well (Supporting Information Fig. S1E and F). As both CD44 and the EGFR could addition-

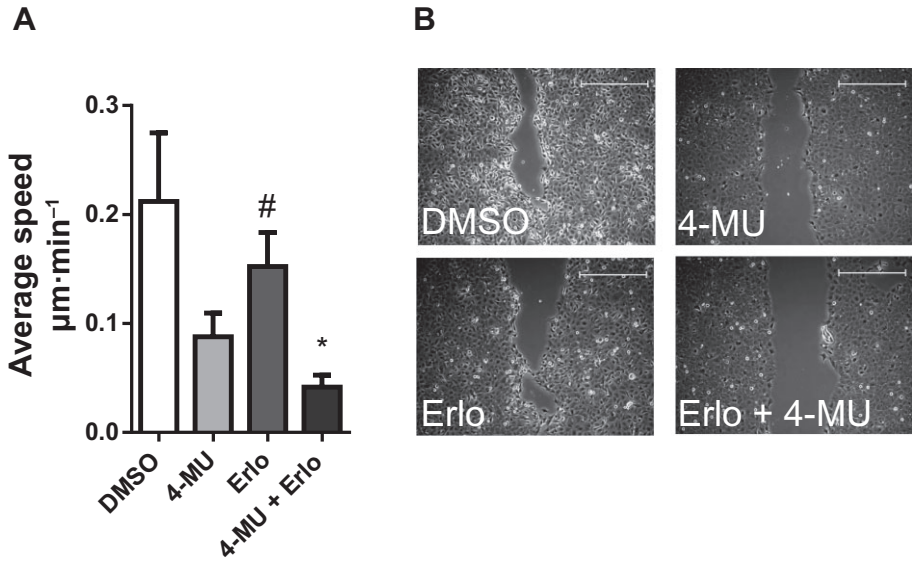

Figure 5

Combined erlotinib and 4-MU treatment attenuated KYSE-410 cell migration. (A) Average velocity of gap closure calculated as the mean speed of the slowest and the fastest migrating front within 24 h, $n = 6$. (B) Representative images taken 10 h after initiation of the migration assay; scale bars indicate 500 µm. Data represent mean ± SEM; *$P < 0.05$ compared with control; #$P < 0.05$ compared with erlotinib + 4-MU.

ally signal via the PI3K/Akt pathway, Akt phosphorylation was analysed. However, after 24 h of treatment, no significant reduction in Akt phosphorylation in any of the treatment groups was observed in KYSE-410 (Supporting Information Fig. S4C and D).

Erlotinib and 4-MU-treated KYSE-410 cells showed impaired migration

The impact of the treatment on cell migration was studied in addition to the anti-proliferative effects of 4-MU and erlotinib. The mean speed of gap closure was significantly lower in erlotinib plus 4-MU-treated KYSE-410 as compared to vehicle or erlotinib-treated cells (Figure 5).

Combined inhibition of EGFR and HAS activity was effective in the 3D cell culture

The efficacy of combining 4-MU and erlotinib was studied in MCTS 3D cell culture of KYSE-410 since a 3D system potentially reflects more realistically the *in vivo* situation regarding metabolic gradients, drug gradients and proliferative gradients and allows for 3D cell–cell and cell–matrix interaction. Starting 4 days after seeding, MCTS were treated with 1 µmol·L^{-1} erlotinib, 300 µmol·L^{-1} 4-MU or a combination of both for 10 days. As depicted in Figure 6A and B, MCTS growth was most effectively suppressed in the double treatment group. Interestingly, erlotinib and 4-MU showed varying efficacy in reducing ERK phosphorylation when comparing two-dimensional (2D) and three-dimensional (3D) cell culture formats. 4-MU led to a significant reduction in ERK phosphorylation after 24 h of treatment in the 3D cell culture, whereas in the 2D cell culture, no significant difference could be observed compared with control (Figures 6C and 4A and B, respectively). However, the combination of erlotinib and 4-MU decreased ERK phosphorylation significantly in either setting. The significantly suppressed ERK phosphorylation by combined erlotinib and 4-MU treatment was detectable after 24 h and lasted for 10 days of treatment (Figure 6C and D).

HAS2 mRNA expression was reduced by 3D cell culture or by erlotinib and 4-MU treatment in 2D cell culture

As 4-MU seemed to act differently in the 2D and 3D cell cultures regarding the phosphorylation of ERK, the expression of HA-related genes and of the EGFR was analysed. 4-MU-treated MCTS had significantly lower HAS2, RHAMM and EGFR mRNA expression and higher HAS3 mRNA expression compared with the 2D cell culture (Figure 7A). In the 2D cell culture, HAS2 mRNA expression was significantly reduced in all treatment groups, and combining erlotinib and 4-MU led to the lowest HAS2 mRNA expression (Figure 7B). Treatment with erlotinib and erlotinib in combination with 4-MU reduced the mRNA expression of HAS3 (Figure 7C). As a result of reduced HAS mRNA expression by erlotinib treatment, decreased amounts of HA in cell culture supernatants were detected (Figure 7E). Additionally, CD44 mRNA expression was reduced by 4-MU and erlotinib alone or in combination.

In contrast to the 2D cell culture, HAS2 and CD44 mRNA expressions were not significantly reduced in the 3D cell culture by any treatment (Figure 7F and H). HAS3 mRNA expression was even increased by the combined erlotinib

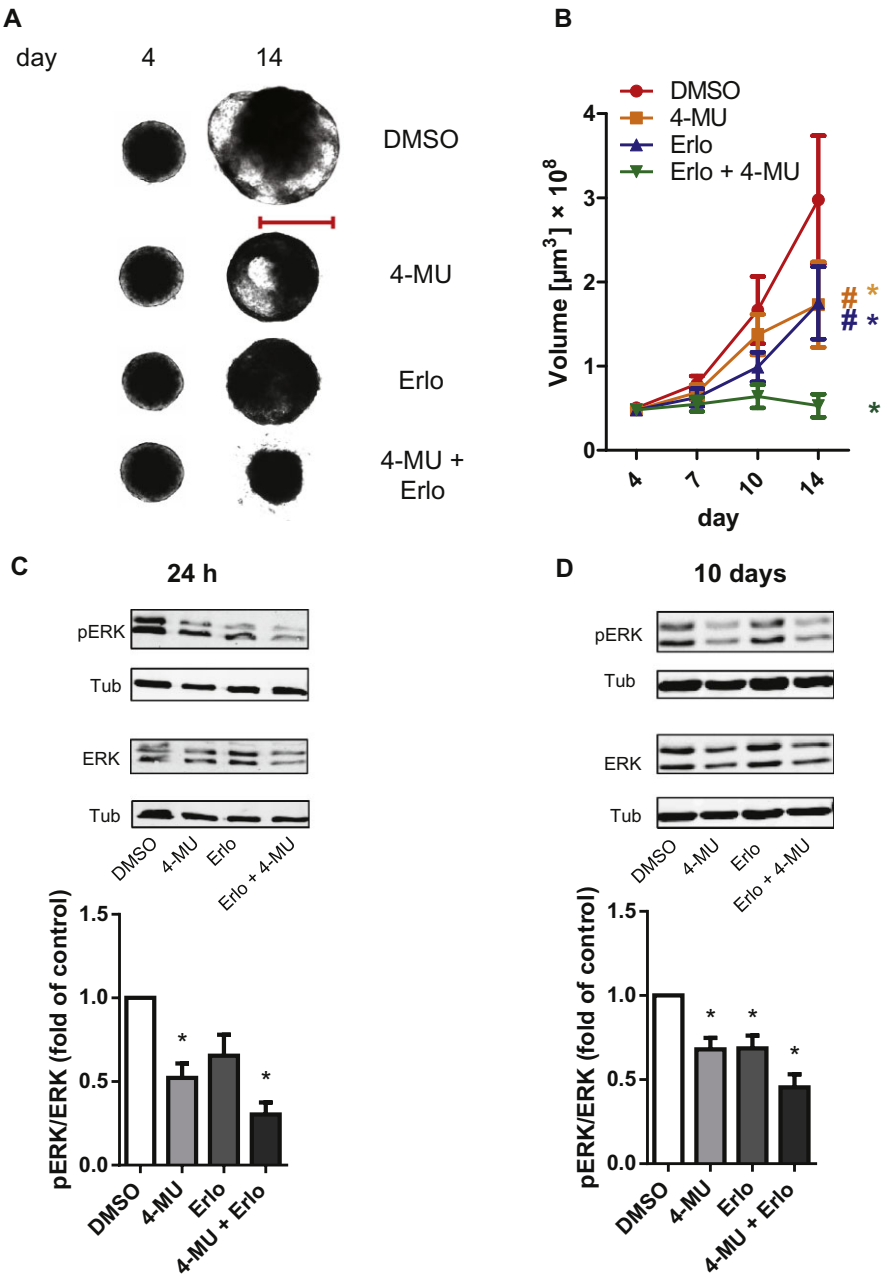

Figure 6

Combined erlotinib and 4-MU treatment inhibited growth of MCTS and ERK phosphorylation in KYSE-410. (A) Representative images of MCTS before (day 4) and after 10 days (day 14) of treatment with vehicle, erlotinib, 4-MU or a combination of 4-MU and erlotinib; scale bar indicates 500 µm. (B) MCTS volumes before (day 4) and after 3, 6, and 10 days of treatment with vehicle, erlotinib, 4-MU or a combination of 4-MU and erlotinib, $n = 6$. (C) ERK phosphorylation in MCTS determined by Western blot after 24 h of treatment with erlotinib and 4-MU as single agents or in combination, $n = 7$. (D) Western blot analysis of phosphorylated ERK in relation to total ERK after 10 days of treatment with vehicle, erlotinib, 4-MU or a combination of 4-MU and erlotinib, $n = 7$. Data are presented as mean ± SEM; *$P < 0.05$ compared with control; #$P < 0.05$ compared with erlotinib + 4-MU.

and 4-MU treatment (Figure 7G). The lack of HAS2 mRNA reduction in the 3D cell culture may be explained by the already low HAS2 mRNA expression in MCTS compared with the 2D cell culture (Figure 7A). The mean relative HAS2 mRNA expression of control-treated MCTS was found to be 0.69 (±0.085 SEM)-fold of that in the combined erlotinib and 4-MU-treated cells in the 2D cell culture (data not shown).

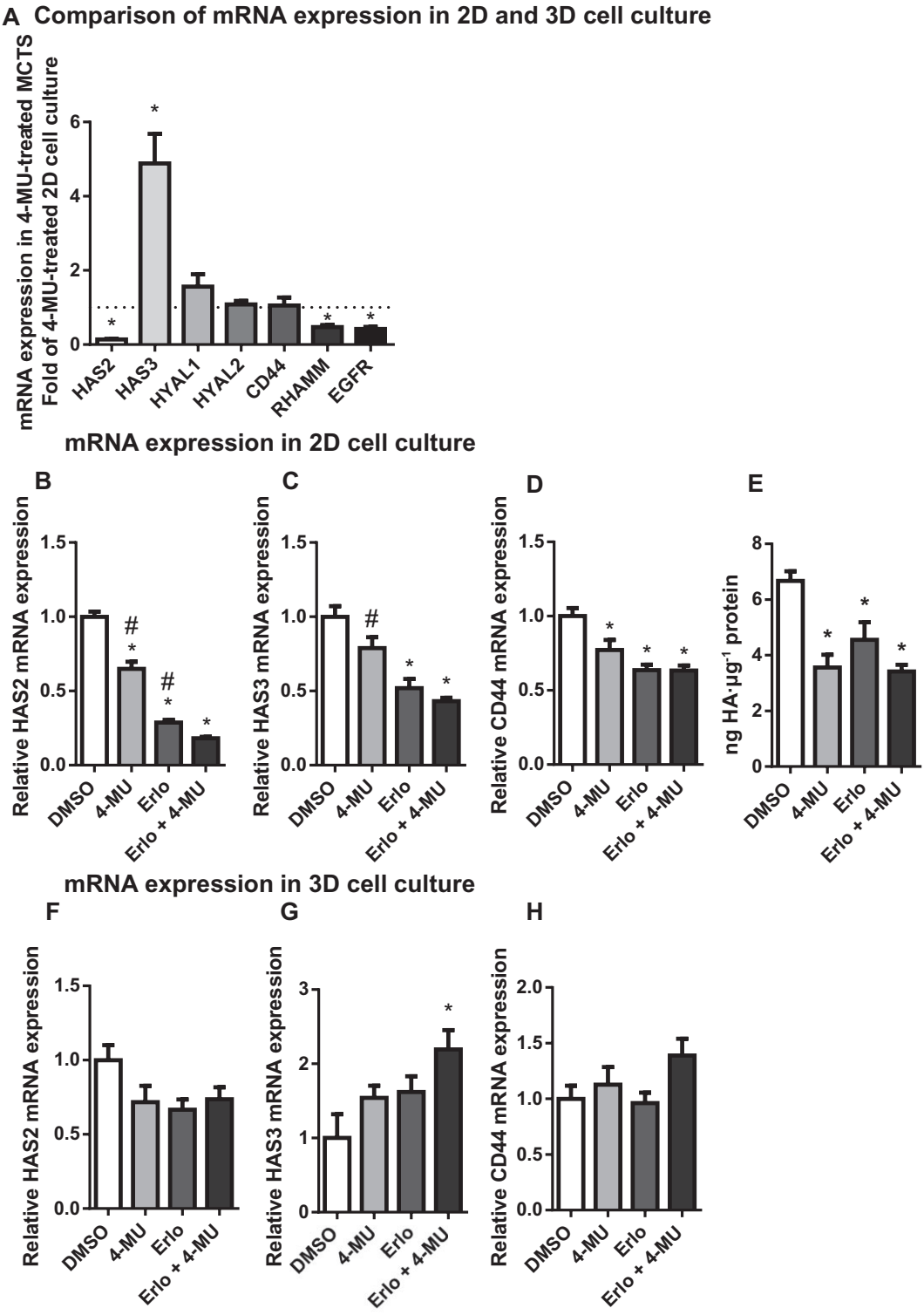

Figure 7

mRNA expression of HA-related genes and EGFR in KYSE-410 in 2D and 3D cell cultures. (A) mRNA expression of HAS, hyaluronidases (HYAL), CD44, RHAMM and EGFR in 4-MU-treated MCTS presented as fold of 4-MU-treated 2D cell culture, $n = 6$. mRNA expression of (B) HAS2 (C) HAS3 and (D) CD44 in the 2D cell culture after 24 h of treatment with vehicle, erlotinib, 4-MU or a combination of 4-MU and erlotinib, $n = 7$. (E) Amount of HA in cell culture supernatants of 4-MU, erlotinib or vehicle-treated KYSE-410 conditioned for 24 h and normalized to total protein, $n = 8$. mRNA expression of (F) HAS2 (G) HAS3 (H) CD44 in MCTS after 24 h of treatment with vehicle, erlotinib, 4-MU or a combination of 4-MU and erlotinib, $n = 6$. Data represent mean ± SEM; *$P < 0.05$ compared with control; #$P < 0.05$ compared with erlotinib + 4-MU.

Discussion and conclusions

Erlotinib is used in advanced or metastatic non-small-cell lung cancer for treatment after chemotherapy and it has recently been approved for first-line treatment of metastatic non-small-cell lung cancers that are characterized by activating EGFR exon 19 deletions or exon 21 substitution mutations. In this patient subgroup, erlotinib treatment was superior to standard chemotherapy. This was not observed in other large trials without stratification for these mutations (Khozin *et al.*, 2014). In ESCC, EGFR mutations are rare (Liu *et al.*, 2011; Gonzaga *et al.*, 2012; Kato *et al.*, 2013) and erlotinib has shown only modest efficacy in clinical trials. Our experiments showed that 4-MU may be an eligible candidate for combination with erlotinib. As an approved choleretic drug, it is well tolerated (Gonzalo-Garijo *et al.*, 1996). We investigated the efficacy of the combination of erlotinib and decreased HA signalling on proliferation, cell migration, MAPK signalling and its efficacy in the 3D cell culture.

Most markedly reduced cell numbers and migration were observed after treatment with the combination of 4-MU and erlotinib. It has previously been demonstrated that both RHAMM and CD44 are involved in proliferative signalling (Twarock *et al.*, 2010). Additionally, both CD44 and RHAMM may interact with growth factor receptors such as EGF and PDGF receptors (Turley *et al.*, 2002; Toole, 2009). This may contribute to an at least by trend augmented effect of erlotinib observed in siCD44 and siRHAMM-transfected cells (Figure 1C and E), although siRNA targeting CD44 or RHAMM alone had no significant effects on cell counts. Alternatively, 4-MU might affect cell growth by additional mechanisms independent of HA synthesis (Nakamura *et al.*, 2007; Edward *et al.*, 2010).

We further investigated the underlying mechanism of the reduced cell number after combined treatment. For this purpose, the cell cycle was analysed and [^{3}H]-thymidine incorporation was quantified after 24 h of treatment. As the proportion of cells in the sub-G1 phase did not change but the proportion of cells in the S-phase was reduced, we concluded that the proliferative activity of cells was decreased and that apoptosis was not affected in KYSE-410, KYSE-270 and KYSE-520. In line with our findings, Sutter *et al*. (2006) did not observe apoptotic effects in ESCC cells treated with erlotinib. However, other investigations report a pro-apoptotic effect of 4-MU (Lokeshwar *et al.*, 2010; Urakawa *et al.*, 2012) or erlotinib (Fichter *et al.*, 2014).

The Akt and ERK pathways are prominent downstream pathways of EGFR and HA signalling and 4-MU alone has been shown to reduce ERK phosphorylation in OSC1 cells (Twarock *et al.*, 2010). In our setting, 4-MU alone was only able to consistently reduce ERK phosphorylation in the 3D cell culture (Figure 6). Also, the strong additional effect of the combination, compared to EGFR TK inhibition alone, on ERK phosphorylation was not seen in the 2D cultures. This may point to an important role of extracellular matrix molecules such as HA in the 3D cell structures. Moreover, 4-MU or erlotinib was reported to additionally decrease Akt phosphorylation (Lokeshwar *et al.*, 2010; Arai *et al.*, 2011; Urakawa *et al.*, 2012; Fichter *et al.*, 2014), which could not be detected in the present experimental set-up.

Furthermore, it is important to test the efficacy of combination of erlotinib and 4-MU in a 3D model of intermediate complexity that is characterized by cellular heterogeneity, nutrient and oxygen gradients and which allows for 3D cell–cell interactions and a 3D extracellular matrix arrangement. Therefore, we established an MCTS growth assay as a model of, that is, tumour micro-regions or micro-metastases (Vinci *et al.*, 2012). Additionally, there may be different efficacies of drugs in monolayer cell culture as compared to the 3D cell culture (Friedrich *et al.*, 2009). In the experiments reported here, not only ERK phosphorylation but also gene expression was differentially regulated in the 3D cell culture. For example, the reduction in HAS2 and CD44 mRNA expression that was observed after 4-MU treatment in other settings (Kultti *et al.*, 2009; Lokeshwar *et al.*, 2010) was only seen in the 2D cell culture. Further research is required to reveal the underlying mechanisms of the differences in ERK activation after 4-MU treatment. Possibly, ERK activation is more sensitive to changes in HA concentration in an environment of low HAS2, RHAMM and EGFR expression that was observed in the 3D cell culture. Importantly, a comparison of the anti-cancer activities of the drugs in the 2D and 3D cell culture, as measured by the cell number or MCTS volume, showed that single agents had moderate but the combination strong effects in both settings.

In order to determine if 4-MU and erlotinib acted in a synergistic or in an additive way, we calculated the CI as described by Chou (2006). We chose the initial cell count experiment as a key finding to evaluate the mutual action. In order to achieve acceptable linear regression coefficients, we used the average effect values of independent experiments to calculate median-effect plots and the CI. In cancer studies, the CI values corresponding to high effects such as ED_{95} are of special interest. In our setting, the value for ED_{95} was calculated to be 0.58 in KYSE-410, 0.59 in KYSE-270 and 0.43 in KYSE-520, thus being in the range of 0.3–0.7, which is defined to describe synergism (Chou, 2006).

The mechanism of the synergistic action of 4-MU and erlotinib remains to be elucidated. In the 2D cell culture, treatment with erlotinib alone effectively decreased ERK phosphorylation even though it was not decreased significantly in all settings investigated. At an earlier time point, 4-MU also tended to inhibit this pathway, which may contribute to the synergism between 4-MU and EGFR inhibition. Furthermore, in some cell lines, the HA-receptor CD44 could interact and activate the EGFR (Toole, 2009) and it may additionally interact with the PDGFR, c-Met, ErbB2 and TGFR (TGFBR1) or cytoskeletal proteins such as ankyrin or adaptor proteins and GTPases, such as, RhoA (Toole, 2009; Misra *et al.*, 2011). Moreover, other receptors such as RHAMM can contribute to HA signalling. A synergistic effect due to a more pronounced inhibition of HA synthesis by combining 4-MU and erlotinib seemed to be unlikely as the amount of HA in cell culture supernatants was not significantly lower in the double treatment group compared to single treatments. Additionally, an HA-independent mechanism of 4-MU action cannot be excluded. Hence, there are several possible mechanisms that could be responsible for the observed synergistic inhibitory effects of erlotinib plus 4-MU on cell number.

The results of the present study show that treatment of ESCC cells with the combination of the EGFR inhibitor erlotinib and the HA synthesis inhibitor 4-MU profoundly inhibits the proliferation and migration of three different ESCC cell lines as well as 3D MCTS growth. Therefore, 4-MU may be a promising agent to increase erlotinib efficacy in ESCC.

Acknowledgements

We thank Ms Petra Rompel for excellent technical assistance. This study was supported by Grant FI682/4-1 from the Deutsche Forschungsgemeinschaft.

Author contributions

I. K., T. F., S. T. and J. W. F. designed the experiments. Experiments were carried out and statistically analysed by I. K. I. K., T. F., S. T. and J. W. F. wrote the manuscript.

Conflict of interest

The authors declare that they have no competing interests.

References

Alexander SPH, Benson HE, Faccenda E, Pawson AJ, Sharman JL, Spedding M *et al*. (2013a). The concise guide to pharmacology 2013/14: catalytic receptors. Br J Pharmacol 170: 1676–1705.

Alexander SPH, Benson HE, Faccenda E, Pawson AJ, Sharman JL, Spedding M *et al*. (2013b). The concise guide to pharmacology 2013/14: enzymes. Br J Pharmacol 170: 1797–1867.

Arai E, Nishida Y, Wasa J, Urakawa H, Zhuo L, Kimata K *et al*. (2011). Inhibition of hyaluronan retention by 4-methylumbelliferone suppresses osteosarcoma cells in vitro and lung metastasis in vivo. Br J Cancer 105: 1839–1849.

Auvinen P, Tammi R, Parkkinen J, Tammi M, Agren U, Johansson R *et al*. (2000). Hyaluronan in peritumoral stroma and malignant cells associates with breast cancer spreading and predicts survival. Am J Pathol 156: 529–536.

Auvinen P, Tammi R, Kosma VM, Sironen R, Soini Y, Mannermaa A *et al*. (2013). Increased hyaluronan content and stromal cell CD44 associate with HER2 positivity and poor prognosis in human breast cancer. Int J Cancer 132: 531–539.

Benitez A, Yates TJ, Shamaldevi N, Bowen T, Lokeshwar VB (2013). Dietary supplement hymecromone and sorafenib: a novel combination for the control of renal cell carcinoma. J Urol 190: 285–290.

Cheng XB, Sato N, Kohi S, Yamaguchi K (2013). Prognostic impact of hyaluronan and its regulators in pancreatic ductal adenocarcinoma. PLoS ONE 8: e80765.

Chou TC (2006). Theoretical basis, experimental design, and computerized simulation of synergism and antagonism in drug combination studies. Pharmacol Rev 58: 621–681.

Chou TC, Martin N (2005). CompuSyn for Drug Combinations: PC Software and User's Guide: A Computer Program for Quantitation of Synergism and Antagonism in Drug Combinations, and the Determination of IC50 and ED50 and LD50 Values. ComboSyn Inc: Paramus, NJ.

Citri A, Yarden Y (2006). EGF-ERBB signalling: towards the systems level. Nat Rev Mol Cell Biol 7: 505–516.

Dragovich T, McCoy S, Fenoglio-Preiser CM, Wang J, Benedetti JK, Baker AF *et al*. (2006). Phase II trial of erlotinib in gastroesophageal junction and gastric adenocarcinomas: SWOG 0127. J Clin Oncol 24: 4922–4927.

Edward M, Quinn JA, Pasonen-Seppänen SM, McCann BA, Tammi RH (2010). 4-Methylumbelliferone inhibits tumour cell growth and the activation of stromal hyaluronan synthesis by melanoma cell-derived factors. Br J Dermatol 162: 1224–1232.

Ferlay J, Soerjomataram I, Dikshit R, Eser S, Mathers C, Rebelo M *et al*. (2015). Cancer incidence and mortality worldwide: sources, methods and major patterns in GLOBOCAN 2012. Int J Cancer 136: E359–E386.

Fichter CD, Timme S, Braun JA, Gudernatsch V, Schöpflin A, Bogatyreva L *et al*. (2014). EGFR, HER2 and HER3 dimerization patterns guide targeted inhibition in two histotypes of esophageal cancer. Int J Cancer 135: 1517–1530.

Friedrich J, Seidel C, Ebner R, Kunz-Schughart LA (2009). Spheroid-based drug screen: considerations and practical approach. Nat Protoc 4: 309–324.

Gonzaga IM, Soares-Lima SC, de Santos PT, Blanco TC, de Reis BS, Quintella DC *et al*. (2012). Alterations in epidermal growth factor receptors 1 and 2 in esophageal squamous cell carcinomas. BMC Cancer 12: 569.

Gonzalo-Garijo MA, Revenga-Arranz F, Moneo-Goiri I (1996). Anaphylactic-type reaction to hymecromone. Allergy 51: 442–443.

Hiraga T, Ito S, Nakamura H (2013). Cancer stem-like cell marker CD44 promotes bone metastases by enhancing tumorigenicity, cell motility, and hyaluronan production. Cancer Res 73: 4112–4122.

Ikuta K, Urakawa H, Kozawa E, Arai E, Zhuo L, Futamura N *et al*. (2014). Hyaluronan expression as a significant prognostic factor in patients with malignant peripheral nerve sheath tumors. Clin Exp Metastasis 31: 715–725.

Ilson DH, Kelsen D, Shah M, Schwartz G, Levine DA, Boyd J *et al*. (2011). A phase 2 trial of erlotinib in patients with previously treated squamous cell and adenocarcinoma of the esophagus. Cancer 117: 1409–1414.

Iyer R, Chhatrala R, Shefter T, Yang G, Malhotra U, Tan W *et al*. (2013). Erlotinib and radiation therapy for elderly patients with esophageal cancer – clinical and correlative results from a prospective multicenter phase 2 trial. Oncology 85: 53–58.

Jonsson EL, Nylander K, Hallen L, Laurell G (2012). Effect of radiotherapy on expression of hyaluronan and EGFR and presence of mast cells in squamous cell carcinoma of the head and neck. Oncol Lett 4: 1177–1182.

Kato H, Arao T, Matsumoto K, Fujita Y, Kimura H, Hayashi H *et al*. (2013). Gene amplification of EGFR, HER2, FGFR2 and MET in esophageal squamous cell carcinoma. Int J Oncol 42: 1151–1158.

Khozin S, Blumenthal GM, Jiang X, He K, Boyd K, Murgo A *et al*. (2014). U.S. Food and Drug Administration approval summary: erlotinib for the first-line treatment of metastatic non-small cell lung cancer with epidermal growth factor receptor exon 19 deletions or exon 21 (L858R) substitution mutations. Oncologist 19: 774–779.

Kultti A, Pasonen-Seppänen S, Jauhiainen M, Rilla KJ, Kärnä R, Pyoria E *et al*. (2009). 4-Methylumbelliferone inhibits hyaluronan synthesis by depletion of cellular UDP-glucuronic acid and downregulation of hyaluronan synthase 2 and 3. Exp Cell Res 315: 1914–1923.

Liu QW, Fu JH, Luo KJ, Yang HX, Wang JY, Hu Y *et al*. (2011). Identification of EGFR and KRAS mutations in Chinese patients with esophageal squamous cell carcinoma. Dis Esophagus 24: 374–380.

Lokeshwar VB, Lopez LE, Munoz D, Chi A, Shirodkar SP, Lokeshwar SD *et al*. (2010). Antitumor activity of hyaluronic acid synthesis inhibitor 4-methylumbelliferone in prostate cancer cells. Cancer Res 70: 2613–2623.

Misra S, Heldin P, Hascall VC, Karamanos NK, Skandalis SS, Markwald RR *et al*. (2011). Hyaluronan-CD44 interactions as potential targets for cancer therapy. FEBS J 278: 1429–1443.

Nakamura R, Kuwabara H, Yoneda M, Yoshihara S, Ishikawa T, Miura T *et al*. (2007). Suppression of matrix metalloproteinase-9 by 4-methylumbelliferone. Cell Biol Int 31: 1022–1026.

Nakazawa H, Yoshihara S, Kudo D, Morohashi H, Kakizaki I, Kon A *et al*. (2006). 4-methylumbelliferone, a hyaluronan synthase suppressor, enhances the anticancer activity of gemcitabine in human pancreatic cancer cells. Cancer Chemother Pharmacol 57: 165–170.

Nicoletti I, Migliorati G, Pagliacci MC, Grignani F, Riccardi C (1991). A rapid and simple method for measuring thymocyte apoptosis by propidium iodide staining and flow cytometry. J Immunol Methods 139: 271–279.

Okuda H, Kobayashi A, Xia B, Watabe M, Pai SK, Hirota S *et al*. (2012). Hyaluronan synthase HAS2 promotes tumor progression in bone by stimulating the interaction of breast cancer stem-like cells with macrophages and stromal cells. Cancer Res 72: 537–547.

Palyi-Krekk Z, Barok M, Isola J, Tammi M, Szollosi J, Nagy P (2007). Hyaluronan-induced masking of ErbB2 and CD44-enhanced trastuzumab internalisation in trastuzumab resistant breast cancer. Eur J Cancer 43: 2423–2433.

Pawson AJ, Sharman JL, Benson HE, Faccenda E, Alexander SP, Buneman OP *et al*.; NC-IUPHAR (2014). The IUPHAR/BPS Guide to PHARMACOLOGY: an expert-driven knowledgebase of drug targets and their ligands. Nucl Acids Res 42 (Database Issue): D1098–D1106.

Rogojina AT, Orr WE, Song BK, Geisert EE Jr (2003). Comparing the use of Affymetrix to spotted oligonucleotide microarrays using two retinal pigment epithelium cell lines. Mol Vis 9: 482–496.

Ropponen K, Tammi M, Parkkinen J, Eskelinen M, Tammi R, Lipponen P *et al*. (1998). Tumor cell-associated hyaluronan as an unfavorable prognostic factor in colorectal cancer. Cancer Res 58: 342–347.

Röck K, Meusch M, Fuchs N, Tigges J, Zipper P, Fritsche E *et al*. (2012). Estradiol protects dermal hyaluronan/versican matrix during photoaging by release of epidermal growth factor from keratinocytes. J Biol Chem 287: 20056–20069.

Shimada Y, Imamura M, Wagata T, Yamaguchi N, Tobe T (1992). Characterization of 21 newly established esophageal cancer cell lines. Cancer 69: 277–284.

Stahl M, Mariette C, Haustermans K, Cervantes A, Arnold D (2013). Oesophageal cancer: ESMO Clinical Practice Guidelines for diagnosis, treatment and follow-up. Ann Oncol 24 (Suppl. 6): vi51–vi56.

Sutter AP, Höpfner M, Huether A, Maaser K, Scherubl H (2006). Targeting the epidermal growth factor receptor by erlotinib (Tarceva) for the treatment of esophageal cancer. Int J Cancer 118: 1814–1822.

Toole BP (2009). Hyaluronan-CD44 interactions in cancer: paradoxes and possibilities. Clin Cancer Res 15: 7462–7468.

Turley EA, Noble PW, Bourguignon LY (2002). Signaling properties of hyaluronan receptors. J Biol Chem 277: 4589–4592.

Twarock S, Röck K, Sarbia M, Weber AA, Janicke RU, Fischer JW (2009). Synthesis of hyaluronan in oesophageal cancer cells is uncoupled from the prostaglandin-cAMP pathway. Br J Pharmacol 157: 234–243.

Twarock S, Tammi MI, Savani RC, Fischer JW (2010). Hyaluronan stabilizes focal adhesions, filopodia, and the proliferative phenotype in esophageal squamous carcinoma cells. J Biol Chem 285: 23276–23284.

Twarock S, Freudenberger T, Poscher E, Dai G, Jannasch K, Dullin C *et al*. (2011). Inhibition of oesophageal squamous cell carcinoma progression by in vivo targeting of hyaluronan synthesis. Mol Cancer 10: 30.

Urakawa H, Nishida Y, Wasa J, Arai E, Zhuo L, Kimata K *et al*. (2012). Inhibition of hyaluronan synthesis in breast cancer cells by 4-methylumbelliferone suppresses tumorigenicity in vitro and metastatic lesions of bone in vivo. Int J Cancer 130: 454–466.

Vinci M, Gowan S, Boxall F, Patterson L, Zimmermann M, Court W *et al*. (2012). Advances in establishment and analysis of three-dimensional tumor spheroid-based functional assays for target validation and drug evaluation. BMC Biol 10: 29.

Wang C, Tammi M, Guo H, Tammi R (1996). Hyaluronan distribution in the normal epithelium of esophagus, stomach, and colon and their cancers. Am J Pathol 148: 1861–1869.

Yoshihara S, Kon A, Kudo D, Nakazawa H, Kakizaki I, Sasaki M *et al*. (2005). A hyaluronan synthase suppressor, 4-methylumbelliferone, inhibits liver metastasis of melanoma cells. FEBS Lett 579: 2722–2726.

Zhai Y, Hui Z, Wang J, Zou S, Liang J, Wang X *et al*. (2013). Concurrent erlotinib and radiotherapy for chemoradiotherapy-intolerant esophageal squamous cell carcinoma patients: results of a pilot study. Dis Esophagus 26: 503–509.

Supporting information

Additional Supporting Information may be found in the online version of this article at the publisher's web-site:

http://dx.doi.org/10.1111/bph.13240

Figure S1 Cell count and ERK phosphorylation in KYSE-410 treated with gefitinib and ERK phosphorylation in KYSE-410 treated with erlotinib and 4-MU for 20 min. (A) KYSE-410 cell count after 72 h of treatment with serial dilutions of gefitinib or 4-MU as single agents or in combination, n = 5. (B) CI values calculated from the means of the cell count data according to the method by Chou (2006). The line-drawing shows the fitted values and actual values are depicted as (●). (C) Western blot analysis of phosphorylated ERK in relation to total ERK in KYSE-410 after 24 h of treatment with gefitinib and 4-MU, n = 7. (D) Representative blots showing phosphorylated and total ERK and β-tubulin loading control

in lysates of KYSE-410. (E) Western blot analysis of phosphorylated ERK in relation to total ERK in KYSE-410 after 20 min of treatment with erlotinib and 4-MU, $n = 6$. (F) Representative blots showing phosphorylated and total ERK and β-tubulin loading control in lysates of KYSE-410. Data are presented as mean ± SEM; $^{*}P < 0.05$ compared to control; $\#P < 0.05$ compared to erlotinib + 4-MU.

Figure S2 Reduced percentage of cells in the S-phase by combined gefitinib and 4-MU treatment in KYSE-410 and by combined erlotinib and 4-MU treatment in KYSE-270 and KYSE-520. Flow cytometric analysis of propidium iodide stained cells treated for 24 h. Depicted are the percentages of gefitinib or 4-MU treated KYSE-410 cells in (A) sub-G1, (B) G0-G1, (C) S, (D) G2-M phase and percentages of erlotinib or 4-MU treated (E–H) KYSE-270 and (I–L) KYSE-520, all $n = 5$. Data are presented as mean ± SEM; $^{*}P < 0.05$ compared to control.